Medical Engineering & Physics 36 (2014) 32–38

Contents lists available at ScienceDirect

Medical Engineering & Physics

journal homepage: www.elsevier.com/locate/medengphy

Design of a flexible fetoscopy manipulation system for congenital diaphragmatic hernia

Wei Yao [a,*], Hariprashanth Elangovan [a], Kypros Nicolaides [b]

[a] Department of Biomedical Engineering, The University of Strathclyde, Glasgow, United Kingdom
[b] Harris Birthright Research Centre for Fetal Medicine, King's College Hospital, Denmark Hill, London, United Kingdom

ARTICLE INFO

Article history:
Received 21 January 2013
Received in revised form 21 August 2013
Accepted 25 August 2013

Keywords:
Fetoscopy
Congenital diaphragmatic hernia
Parallel mechanism

ABSTRACT

Recent advancements in fetal surgery have proven that tracheal occlusion in fetuses with congenital diaphragmatic hernia is an effective way to prevent the occurrence of pulmonary hypoplasia. A novel flexible fetoscope with a parallel mechanism structure of a thumbstick to carry on the fetal tracheal balloon occlusion by the targeting and manipulation of the fetal endoscope at a high standard of quick response and dexterity is proposed in this paper. This design is compared with a commercial rigid fetoscope in terms of operation timing and reduced stress to the fetus at neck level. Experiments using a phantom have demonstrated that the flexible fetoscope has a better dexterity and is able to perform stable tracheoscopy and balloon inflation at different levels of the trachea, with the help of a fiberoptic camera.

1. Introduction

Congenital diaphragmatic hernia (CDH) occurs in about 1/4000 live births. The intrathoracic displacement of the fetal liver and bowel compresses the lungs and impairs their development. This often results in neonatal death from respiratory insufficiency due to pulmonary hypoplasia and hypertension (Fig. 1).

In the last twenty years, several attempts have been made to carry out fetal surgery to prevent the abnormal development of the fetal lungs. Initially, open fetal surgery was carried out, which involved laparotomy and hysterotomy with partial birth of the fetus for thoracotomy and repair of the diaphragmatic defect [1,2]. Recently, a minimally invasive technique has been developed and this has replaced open fetal surgery [3–5]. A rigid fetoscope is introduced into the uterus and then into the fetal mouth, oropharynx and trachea. A balloon is then used to occlude the trachea and prevent the escape of lung secretions. The resulting increase in pressure and stretching of the lungs stimulates lung growth [6,7]. The balloon is usually inserted at around 26 weeks and removed by a second fetoscopic procedure at 34 weeks, which involves bursting the balloon.

The use of a rigid fetoscope, as seen in Fig. 2, necessitates a series of manipulations to achieve hyperextension of the fetal neck and subsequently to direct the endoscope under the epiglottis in order to visualize the vocal cords. Using a rigid fetoscope for such procedures produces an increased stress on the cervical vertebrae or the neck joint of the fetus. Such an abnormal neck posture may result in increased stress on the cervical vertebra, discomfort to the fetus and difficulty in the surgical procedure and it may also result in unprecedented injuries to the delicate structures of the fetus. Moreover, handling a rigid fetoscope for the procedure would demand great surgical skill and hand-eye co-ordination.

The research is about the development of a flexible hand manipulated fetoscope with parallel axis control for increased stability, dexterity and ease of manipulation. Such a system can be manipulated and steered into the trachea of the fetus without injuring the fragile fetal structures and in a way that reduces the tediousness of the surgical process.

2. Methods

A traditional endoscope uses a multi-cable driven system to manipulate the bending of the section tip. The distal tip of the endoscope is controlled by pulling wires attached at the tip and passing the back through the length of the endoscopic shaft to the two angulation control wheels on the control head. This current instrument is less excellent in its performance and requires further development of endoscopy for its serial type controlling mechanism. Based on a high level of dynamic properties, high accuracy, and quick response, a parallel mechanism can be considered in an endoscope for distal tip controlling [8].

This parallel mechanism, due to its significant advantages in terms of its high stiffness, accurate positioning, high speed, and capacity for acceleration, has been widely used in precision surgical tools [9]. For instance, Merlet accomplished an optimal design for a parallel mechanism MIPS (micro parallel structure) at the tip

* Corresponding author. Tel.: +44 01415483030.
E-mail addresses: w.yao@strath.ac.uk, wyao04@gmail.com (W. Yao).

1350-4533/$ – see front matter © 2013 IPEM. Published by Elsevier Ltd. All rights reserved.
http://dx.doi.org/10.1016/j.medengphy.2013.08.014

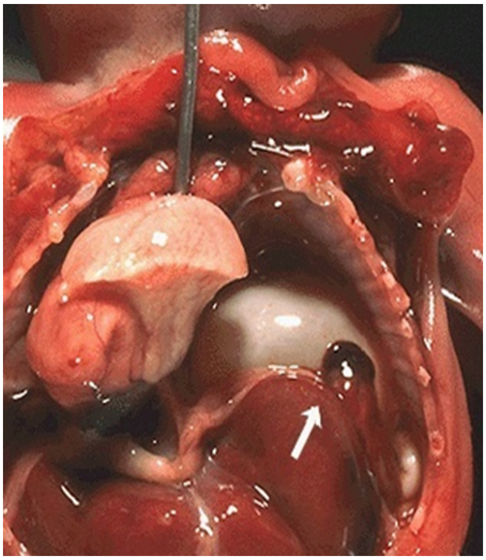

Fig. 1. Fetus with congenital diaphragmatic hernia.

of an endoscope in 2002 [10]. A redundantly actuated 3-UPU parallel mechanism for ankle rehabilitation has been studied in 2008 and 2009 [11,12]. A control algorithm for endoscopy with a simplified Stewart mechanism was explored by Wedlandt and Sastry in the University of California [13]. Also, such MIPS mechanism can be adapted in future to match the needs of other fetal surgeries like meningomyelocoele repair [14].

This paper describes a novel flexible fetoscopic system which has been developed from scratch, controlled by a thumbstick manipulator with a parallel mechanism. The design of this new type of flexible fetoscope is investigated and discussed. The geometry and also the analytic formulae of the relation between the thumbstick input and the distal section output are presented. Ultrasound guided experiments are used to demonstrate the better functionality of the flexible fetoscope when compared to the currently available rigid fetoscope.

2.1. Design of a flexible fetoscope

The flexible fetoscope is composed of a 30,000 Pixel – definition CCD/CMOS based micro-camera unit 1.2 mm in diameter and an optical fiber consisting of a thin tube which can be divided into a more flexible part attached to a probe in the bending section and a less flexible part which serves as a shaft. As illustrated in Fig. 3, the fetoscope control system can be considered to be composed of three parts: a thumbstick which contains a parallel mechanism, a shaft and a bending section attached to a probe which is more flexible. The bending section and part of the shaft gains access to the mouth of the fetus, while the thumbstick control system is manipulated outside the mother's uterus. The thumbstick interface is denoted as a hemisphere, as shown in Fig. 3. The terminal surface is the surface of the micro-probe in the bending section, which would carry the optical fiber based camera and the inflatable balloon.

In minimally invasive tracheal occlusion, the fetoscope is driven by the manually-controlled thumbstick. So the inputs of the fetoscope are the two rotation angles of the thumbstick interface and the output is the position of the fetoscope tip. The intermediary of the two above mentioned sections is the length of the three connecting wires. The connecting wires are 0.2 mm in diameter and are made of titanium having a maximum elongation of 1.785 mm for 20 Newtons of force applied. Since the procedure is USG guided, the surgeon can manipulate the thumbstick and can easily add more pressure to achieve the position required. So the position of the tip of the fetoscope can be calculated by the output of the parallel mechanism in the thumbstick indirectly and the error induced by elasticity can be easily corrected.

The diagram in Fig. 4 provides the design of the construction of the thumbstick. The mechanism can be considered as a 3-UPU (Universal Prismatic Universal) parallel manipulator mechanism with a central strut. The thumbstick interface directly controlled by the human thumb serves as the platform for the parallel mechanism. The cylinder handle acts as the base and support of the parallel mechanism. Each rigid wire is regarded as a limb which acts as a

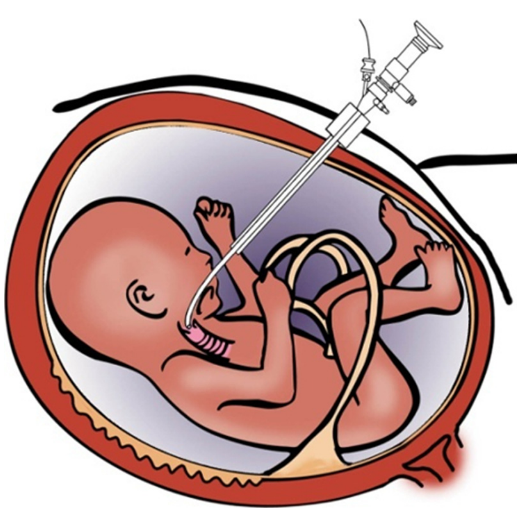

Fig. 2. Process of tracheal intubation using a rigid fetoscope.

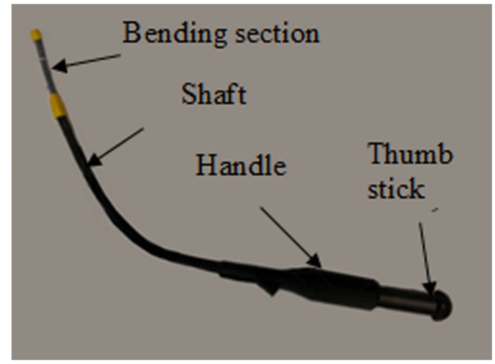

Fig. 3. Construction of the flexible fetoscope.

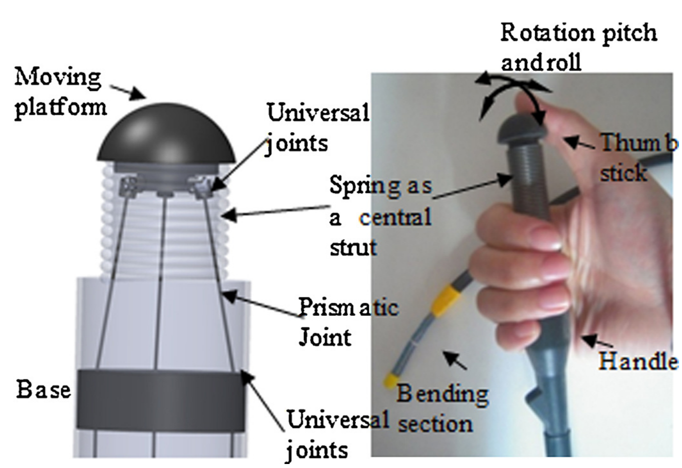

Fig. 4. Construction of the thumbstick.

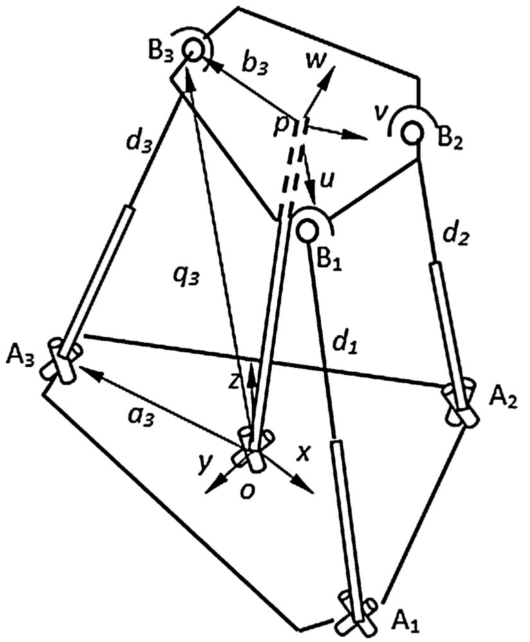

Fig. 5. Geometry of the parallel manipulator in flexible-fetoscopy.

connector to the base and the moving platform by means of a universal joint, a prismatic joint and another universal joint, one after the other, constituting the wire structure. The mechanical spring of the central line of the spring does not change during the bending so that it can be used in the place of a central strut connecting the platform and the base with two universal joints.

2.2. Thumbstick geometry

The geometry of the thumbstick is shown in Fig. 5. Three limbs link the base platform at points A_1, A_2 and A_3 and a moving platform at points B_1, B_2 and B_3, respectively. Two Cartesian coordinate systems $A(x,y,z)$ and $B(u, v, w)$ are attached to the base and the moving platform. The origin O of the fixed coordinate system is attached at the center point of $\Delta A_1A_2A_3$ and the x-axis points in the direction of $\overline{OA_1}$. The z-axis is perpendicular to the $A_1A_2A_3$ plane and the y-axis is defined by the right hand rule. Similarly, the origin P of the moving coordinate system is attached at the center point of $\Delta B_1B_2B_3$ and the u-axis points in the direction of $\overline{PB_1}$. w-axis is perpendicular to the $B_1B_2B_3$ plane and the v-axis is defined by the right hand rule. The limb connects the moving platform and the fixed platform. In each limb there is a universal joint and a prismatic joint. The length of the limbs are defined by $d_i(i=1, 2, 3)$. Two manually actuated angles α and β are used by the surgeon to control the length of the three wires d_1, d_2 and d_3.

The transformation from the moving platform to the base can be described by a position vector $\mathbf{p} = \overline{OP}$, and a 3×3 rotation matrix $^{\mathbf{A}}\mathbf{R_B}$. Let $\boldsymbol{u}$, $\boldsymbol{v}$ and $\boldsymbol{w}$ be three unit vectors defined along the u, v and w axes of the moving coordinate system $B(u, v, w)$, respectively. Then the rotation matrix can be expressed in terms of the direction cosines of $\boldsymbol{u}$, $\boldsymbol{v}$ and $\boldsymbol{w}$ as:

$$^{\mathbf{A}}\mathbf{R_B} = \begin{bmatrix} u_x & v_x & w_x \\ u_y & v_y & w_y \\ u_z & v_z & w_z \end{bmatrix} \quad (1)$$

The three rotation angles γ, β and α are defined as the yaw, pitch and roll about the z, y and x axes.

As the parallel mechanism mentioned before, the universal joints of the central strut constrain rotation about z-axis of the platform. The rotation angle γ is zero. Thus, the rotation matrix with two input angles α and β is expressed in Eq. (2).

$$R(\beta, \alpha) = \begin{bmatrix} \cos\beta & 0 & \sin\beta \\ \sin\alpha\sin\beta & \cos\alpha & -\sin\alpha\cos\beta \\ -\cos\alpha\sin\beta & \cos\alpha & \cos\alpha\cos\beta \end{bmatrix} \quad (2)$$

The position vectors $\mathbf{a}_i(i=1, 2, 3)$ and $^{\mathbf{B}}\mathbf{b}_i(i=1,2,3)$ of point $A_i=(i=1, 2, 3)$ and $B_i=(i=1, 2, 3)$ in the coordinate systems $A(x,y,z)$ and $B(u,v,w)$ are given by:

$$\mathbf{a}_1 = [m, 0, 0]^T \quad (3a)$$

$$\mathbf{a}_2 = \left[-\frac{1}{2}m, \frac{\sqrt{3}}{2}m, 0\right]^T \quad (3b)$$

$$\mathbf{a}_3 = \left[-\frac{1}{2}m, -\frac{\sqrt{3}}{2}m, 0\right]^T \quad (3c)$$

and

$$^{\mathrm{B}}\mathbf{b}_1 = [h, 0, 0]^T \quad (4a)$$

$$^{\mathrm{B}}\mathbf{b}_2 = \left[-\frac{1}{2}h, \frac{\sqrt{3}}{2}h, 0\right]^T \quad (4b)$$

$$^{\mathrm{B}}\mathbf{b}_3 = \left[-\frac{1}{2}h, \frac{\sqrt{3}}{2}h, 0\right]^T \quad (4c)$$

The position vector $\mathbf{q}_i(i=1,2,3)$ of point $B_i(i=1,2,3)$ with respect to the fixed coordinate system $A(x,y,z)$ can be obtained by the following expression:

$$\mathbf{q}_i = \mathbf{p} + {}^{\mathbf{A}}\mathbf{R_B}{}^{\mathbf{B}}\mathbf{b}_i \quad (i=1,2,3) \quad (5)$$

where p_x, p_y and p_z stand for the three components of position vector $\mathbf{p}$.

The length $d_i(i=1, 2, 3)$ can be expressed as follows:

$$d_i^2 = (\mathbf{a}_i - \mathbf{q}_i)^2 \quad (i=1,2,3) \quad (6)$$

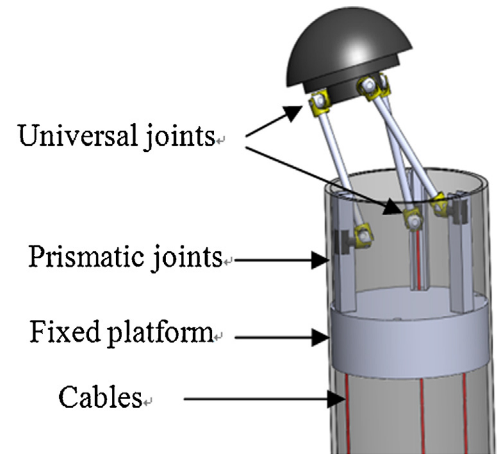

Fig. 6. Construction of the optional parallel manipulator.

2.3. An optional design for the thumbstick mechanism

In the design progress, different types of structure for the thumb designs have been considered. The second architecture, called a 3-PUU manipulator with parallel sliders, is shown in Fig. 6. This manipulator also consists of a moving platform, a fixed base, three

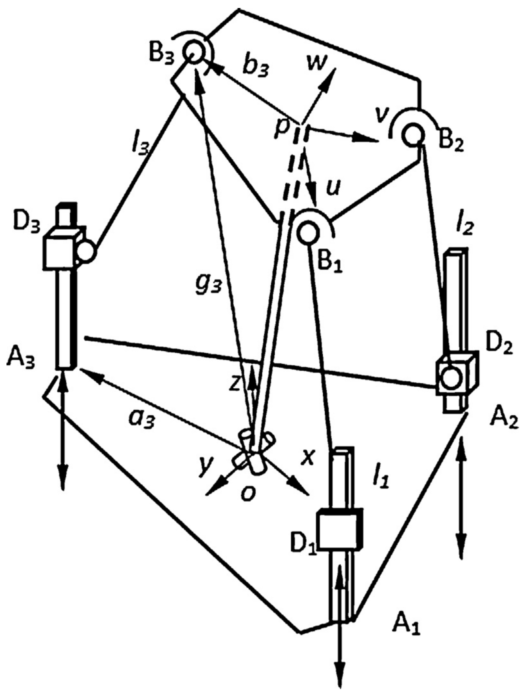

Fig. 7. Geometry of the optional parallel manipulator.

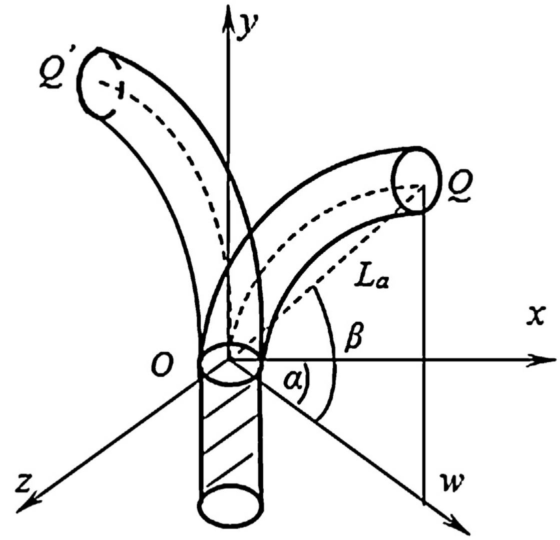

Fig. 8. Configuration of the bending section.

limbs and a central strut. Each limb with the same length connects the fixed base to the moving platform by a prismatic joint followed by two universal joints. The wires which control the position of the tip connect the tip of the fetoscope and the prismatic joints at the limbs. The outputs of this mechanism are the changes of the three prismatic joints' lengths.

The geometry of the 3-PUU parallel manipulator is shown in Fig. 7. As with the 3-UPU in the last section, the position vectors $a_i (i = 1, 2, 3)$ and ${}^{B}\mathbf{b}_i (i = 1, 2, 3)$ of points $A_i (i = 1, 2, 3)$ and $B_i (i = 1, 2, 3)$ in the coordinate systems $A(x,y,z)$ and $B(u,v,w)$ are given by:

$$\mathbf{a}_1 [n, 0, 0]^{\mathrm{T}} \tag{7a}$$

$$\mathbf{a}_2 \left[-\frac{1}{2}n, \frac{\sqrt{3}}{2}n, 0 \right]^T \tag{7b}$$

$$\mathbf{a}_3 \left[-\frac{1}{2}n, \frac{\sqrt{3}}{2}n, 0 \right]^T \tag{7c}$$

and

$$^{\mathrm{B}}\mathbf{b}_1 = [k, 0, 0]^T \tag{8a}$$

$$^{\mathrm{B}}\mathbf{b}_2 = \left[-\frac{1}{2}k, \frac{\sqrt{3}}{2}k, 0 \right]^T \tag{8b}$$

$$^{\mathrm{B}}\mathbf{b}_3 = \left[-\frac{1}{2}k, \frac{\sqrt{3}}{2}k, 0 \right]^T \tag{9c}$$

The position vector $\mathbf{g}_i (i = 1, 2, 3)$ of point $B_i (i = 1, 2, 3)$ with respect to the fixed coordinate system $A(x,y,z)$ can be obtained by the following expression:

$$\mathbf{g}_i = \mathbf{p} + {}^{\mathbf{A}}\mathbf{R}_{\mathbf{B}}{}^{\mathbf{B}}\mathrm{b}_i \quad (i = 1, 2, 3) \tag{10}$$

The length $d_i (i = 1, 2, 3)$ can be expressed as follows:

$$l_i^2 = (\mathbf{a}_i - \mathbf{g}_i)^2 \quad (i = 1, 2, 3) \tag{11}$$

2.4. Configuration of the distal section

In Fig. 8, the base surface is defined as the intersecting surface of the bending section and the connecting wires. The bending section can be considered as the bending starts from the base surface. There are three pulling wires that drive the terminal surface to the required position. When the lengths of the three wires change, the bending section with the camera is driven into different positions. The terminal surface always bends toward the direction of the shorter wires with a constant radius. Thus, the shorter wires pull the tip of the fetoscope into the desired position.

The coordinate system $O(x,y,z)$ is assumed to be as follows. The origin point O is coincident with the geometrical center of the intersecting surface on the base. The plane where the bending section is located is the bending plane which is perpendicular to the x–y plane.

The shortest, medium and longest wires intersect the tip surface at Q_1, Q_2 and Q_3, respectively. Point Q is denoted as the center point of the terminal surface. The position of $Q\,(q_x, q_y, q_z)$ of the terminate surface can be described by two angles β and α, as illustrated in Fig. 8. α demonstrates the angle between the bending plane and the x–y plane. β denotes as the angle between the line from the centroid C of the base surface to the centroid Q of the terminate surface and its projection in the z–x plane. The configuration of the distal section is illustrated in Fig. 8.

La represents the distance from the centroid O of the base surface to the center point Q of the terminate surface. The maximum length of the three pulling wires under the bending deformation in the bending section is

$$l_{\max} = \Delta d_{\max} + l \tag{12}$$

where $\Delta d_{\max} = \max(d_i - d)\ (i = 1, 2, 3)$ is the maximum difference between the ith $(i = 1, 2, 3)$ limb length with deformation and the ith $(i = 1, 2, 3)$ limb length without deformation in the thumbstick, and l is the length of the pulling wire without deformation.

d is the diameter of the distal section. From Fig. 9, the distance *La* from the centroid O of the base surface to the centroid Q of the

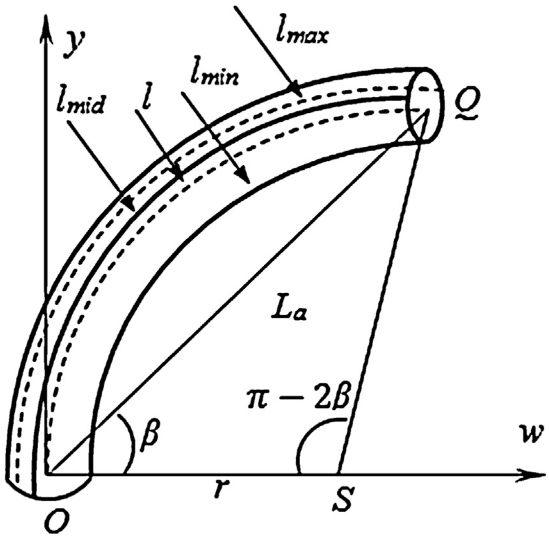

Fig. 9. Flexible tip with deformation in the bending plane.

terminate surface are obtained by the triangle relation of triangle ΔSOQ.

$$La = \sqrt{r^2 + r^2 - 2r^2\cos(\pi - 2)} = \sqrt{2\frac{l^2}{(\pi - 2\beta)^2}[1 - \cos(\pi - 2\beta)]} \tag{13}$$

r is the constant radius of the bending deformation.

Among the three pulling wires, there can be two wires having the same length. The flexible tip is driven by two longer wires with the same length and one shorter wire. The tip bends toward the shorter wire. When one of the longer wires becomes shorter, the tip twists along the y axis toward the shorter wire. The bending surface is in the middle of the two shorter wires. There might be a third special situation for the distal section, which is that the three wires might have equivalent lengths. In this case, deformation does not happen to any of the wires as they are constrained by the central strut design in the thumbstick.

3. Results

3.1. The fetoscopic manipulation system

3.1.1. System overview

Comparing to the first structure in Fig. 4, the second design in Fig. 6 shows a better reliability but less workspace. The first design in Fig. 4 was chosen to develop a prototype. Fig. 4 shows the parallel thumbstick manipulator system, which is proposed to enable the control of the flexible tip of the fetoscope manually by the surgeon with a high level of dexterity. The fetoscope and the manipulator are inserted into the uterus and imaging via the fetoscope and ultrasound is used to navigate with the manipulator, in order to place the DSB (detachable silicone balloon) in the fetal trachea. Finally, the fetal trachea is occluded using the DSB to increase the pressure in the fetal lung. Our approach involves developing an inexpensive, simple and thin flexible manipulator for easier and swifter balloon insertion. The length of the tracheal intubation element is calculated by having 6 cm as a constant minimum value of the endotracheal flexible tube length and adding 1 cm to every 1 kg increment in the weight of the fetus. Since the fetus weighs approximately 600–1 kg at 24–36 weeks, the flexible tip length required would be 7 cm approximately. Hence the proposed fetoscope can be used on the fetus any time after it is 24 weeks old. Certain devices,

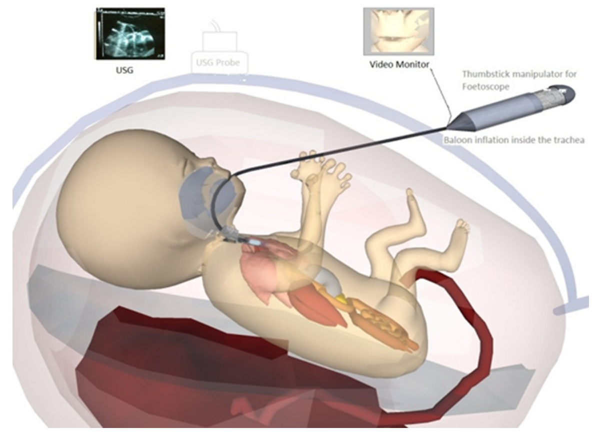

Fig. 10. System overview – flexible fetoscope insertion under USG and live video monitoring and guidance.

both rigid and inflatable, have been tried for immobilization of the fetus which may be used in addition to using this device [15].

3.1.2. Design of the manipulator

The outer diameter of the manipulator's shaft is designed to be 4.50 mm so that the manipulator can be inserted into a 20 F (6.60 mm) trocar. The length of the flexible tip is 70 mm a design based on the neonatal ET (Endo Tracheal) Intubation requirements for a neonate of weight 1 kg. Since the incision in the uterus is very small, the incision need not be sutured, since the contractive force of the uterus itself closes the small hole unaided. Besides, the smaller incision is necessary to avoid premature rupturing of the chorioamniotic membrane, given its poor healing ability.

The developed manipulator uses a parallel axis metal rod driven mechanism to achieve three bending degrees of freedom, using a stable flexible shaft control system acting as a tensigrity structure for improved dexterity and control.

3.2. Procedure overview

The flexible fetoscope is introduced into the uterus and then into the fetal mouth, oropharynx and trachea with the fetus in its anatomical position, as shown in Fig. 10. In contrast to the technique used in rigid fetoscope insertion, where a series of fetal manipulations were required, the use of a flexible fetoscope would require only the manipulation of the thumbstick to facilitate the bending and steering of the manipulation system, as seen in Fig. 11. The surgeon manipulates the fetoscope using the thumbstick to reach the mouth of the fetus initially and steers it further into the oropharynx, visualizing the esophagus and the trachea and manipulates the flexible tip into the trachea. When the desired position is reached, the balloon inflation is done. The entire procedure would be

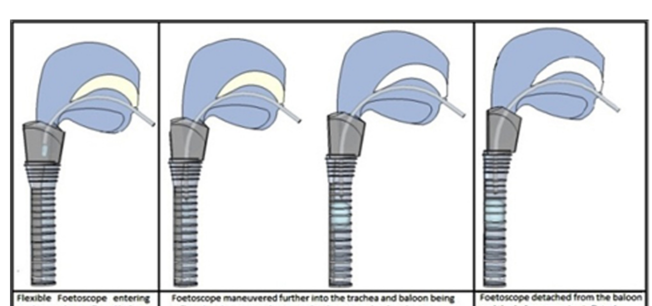

Fig. 11. Process of balloon inflation using a flexible fetoscope.

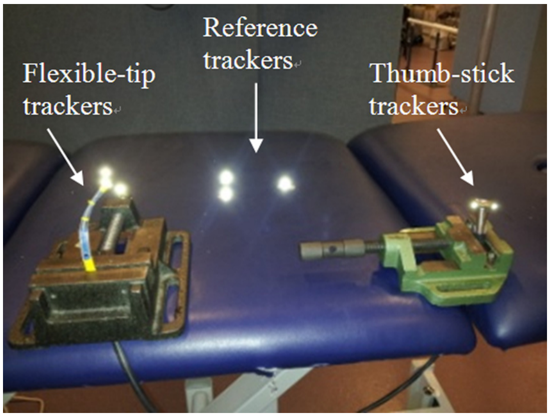

Fig. 12. Optitrack setup for the flexible fetoscope motion tracking.

controlled by the thumbstick manipulation co-ordinated and guided by ultrasound imaging and the video images from the fetoscope.

3.3. Dexterity analysis using an opti-track system

The dexterity analysis of the thumbstick system was carried out with the help of an Optitrack motion tracking system in Fig. 12 at 100 Hz, with the help of IR microtrackers placed on the thumbstick and the flexible tip. The thumbstick end and the tip end trackers were grouped in the optitrack software as mobile rigid bodies and a set of trackers were placed on a plane surface to set the reference plane. The thumbstick was manipulated manually and the corresponding displacement of the flexible tip trackers was tracked with reference to the thumbstick trackers.

In the graph Fig. 13, the net displacement of the trackers on the thumbstick has been compared to those on the flexible tip with reference to the time for every 10 milliseconds. The average time difference between the thumbstick controller and the tip for the motion transmission has been estimated to be 330 microseconds approximately. Hence it is evident that the system operation is well within the time frame required to carry out the procedure using a flexible fetoscope.

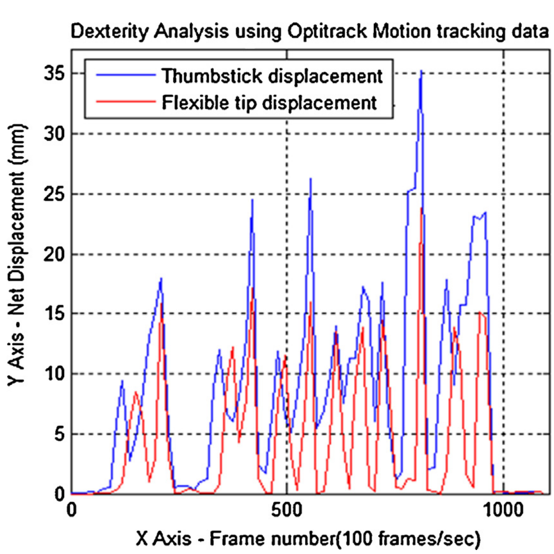

Fig. 13. Dexterity analysis using Optitrack motion tracking data.

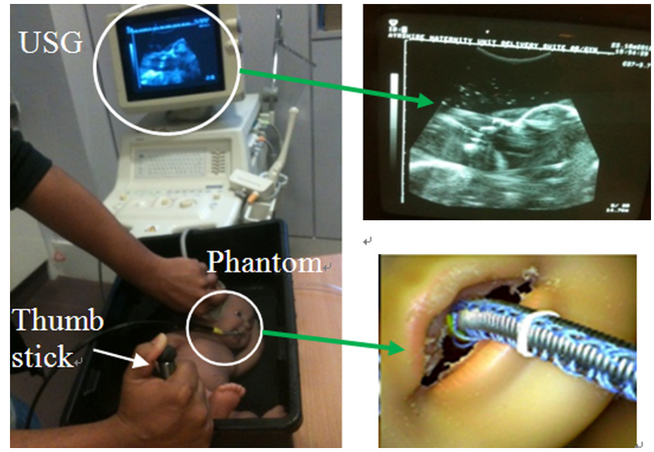

Fig. 14. Ultrasound guided fetoscope insertion with thumbstick control.

3.4. Testing the system on a fetal phantom

The methodology of experimentation is shown in Fig. 14. A latex fetal phantom was used with similar specifications of a 25 week old fetus placed in a latex bladder filled with water placed inside a plastic tub. An ultrasound is then carried out and the nose of the phantom is found. An incision of 4.5 mm is made on the latex wall with the nose of the phantom as the point of reference. The fetoscope was inserted through the incision made on a transparent latex bladder to simulate the layers of the abdominal wall and the uterus.

The mouth of the fetus is visualized using the images transmitted by the USG to the screen and then the flexible tip of the fetoscope is manipulated with the help of the thumbstick control and inserted inside the mouth of the phantom. The tracheal and the esophageal openings are identified, just as in real-time fetal surgery, and then, using careful manipulation of the flexible tip, the fetoscope is inserted into the trachea and then at the desired level a balloon inflation can be performed.

4. Conclusions

This paper has presented an analytical model of a flexible fetoscopy for use with CDH and it has compared the effectiveness of such a system with a rigid fetoscope in reducing the stress on the fragile fetal structures. A novel model of a thumbstick parallel manipulation mechanism, a combination of three universal joints connected to a wire-driven bending tip has been produced, which will result in high levels of dexterity and ease of use for the surgeon.

The study has presented for the first time a way of analyzing the thumbstick based on the parallel mechanism. The thumbstick control parameters were converted into tip control parameters which would produce the required tip operation. The study was demonstrated using a novel dexterous thumbstick with a flexible fetoscope.

The procedure used in CDH surgery was simulated by using a fetal phantom under water under ultrasound guidance and the intubation procedure was successfully performed by the manipulation of the thumbstick without having to change the anatomical position of the head of the fetal phantom. Hence we can conclude that such a flexible fetoscopic manipulator can be used in CDH without requiring any sort of head manipulation or causing injury to the surrounding fetal soft tissues.

Acknowledgment

The first author thanks Professor Guang-Zhong Yang for his support when the author worked in the Department of Surgery and Cancer at Imperial College London.

Conflict of interest statement

None declared.

References

[1] Harrison MR, Adzick NS, Flake AW, Jennings RW, Estes JM, MacGillivray TE, et al. Correction of congenital diaphragmatic hernia in utero: VI. Hard-earned lessons. J Pediatr Surg 1993;28:1411–7.
[2] Harrison MR, Scott Adzick N, Longaker MT, Goldber JD, Rosen MA, Filly RA, et al. Successful repair in utero of a fetal diaphragmatic hernia after removal of herniated viscera from the left thorax. N Engl J Med 1990;322:1582–4.
[3] Deprest J, Gratacos E, Nicolaides KH. On behalf of the FETO task group. Fetoscopic tracheal occlusion (FETO) for severe congenital diaphragmatic hernia: evolution of a technique and preliminary results. Ultrasound Obstet Gynecol 2004;24:121–6.
[4] Deprest JA, Flake AW, Gratacos E, Ville Y, Hecher K, Nicolaides K, et al. The making of fetal surgery. Prenat Diagn 2010;30:653–67.
[5] Deprest JA, Nicolaides K, Gratacos E. Fetal surgery for congenital diaphragmatic hernia is back from never gone. Fetal Diagn Ther 2011;29:6–17.
[6] DiFiore JW, Fauza DO, Slavin R, Peters CA, Fackler JC, Wilson JM. Experimental fetal tracheal ligation reverses the structural and physiological effects of pulmonary hypoplasia in congenital diaphragmatic hernia. J Pediatr Surg 1994;29:248–56 [discussion 256–7].
[7] Bratu I, Flageole H, Laberge JM, Chen MF, Piedboeuf B. Pulmonary structural maturation and pulmonary artery remodeling after reversible fetal ovine tracheal occlusion in diaphragmatic hernia. J Pediatr Surg 2001;36:739–44.
[8] Tsai L. Robot analysis. The mechanics of serial and parallel manipulators. New York: John Wiley & Sons, Inc.; 1999. p. 116–7.
[9] Lu Y, Ding L, Yu J. Autoderivation of topological graphs for type synthesis of planar 3DOF parallel mechanisms. ASME J Mech Rob 2010;2, 011002_1–10.
[10] Merlet JP. Optimal design for the micro parallel robot MIPS. In: Proceedings of the 2002 IEEE international conference on robotics & automation, Washington, DC. 2002. p. 1149–54.
[11] Saglia JA, Dai JS, Galdwell DG. Geometry and kinematic analysis of a redundantly actuated parallel mechanism that eliminates singularities and improves dexterity. ASME J Mech Des 2008;130(12), 124501_1–5.
[12] Saglia JA, Tsagarakis NG, Dai JS, Galdwell DG. Inverse-kinematics-based control of a redundantly actuated platform for rehabilitation. Proc IMechE Part I J Syst Control Eng 2009;223:53–70.
[13] Wendlandt JM, Sastry SS. Design and control of a simplified Stewart platform for endoscopy. In: Proc 33rd IEEE Conf Decision Control, vol. 1. 1994. p. 357–62.
[14] Aaronson OS, Tulipan NB, Cywes R, Sundell HW, Davis GH, Bruner JP, et al. Robot-assisted endoscopic intrauterine myelomeningocele repair: a feasibility study. Pediatr Neurosurg 2002;36:85–9.
[15] Liao H, Suzuki H, Matsumiya K, Masamune K, Dohi T, Chiba T. Fetus supporting flexible manipulator with balloon-type stabilizer for endoscopic intrauterine surgery. Int J Med Robot Comput Assist Surg 2008;4:214–23.